Research Article | Vol. 25, No. 24 | 27 Nov 2017 | OPTICS EXPRESS 29874
Optics EXPRESS

Comparison of nematic liquid-crystal and DMD based spatial light modulation in complex photonics

SERGEY TURTAEV,[1,2,3] IVO T. LEITE,[1,3] KEVIN J. MITCHELL,[4] MILES J. PADGETT,[4] DAVID B. PHILLIPS[4,5] & TOMÁŠ ČIŽMÁR[1,3,6,*]

[1]School of Science and Engineering, University of Dundee, Nethergate, Dundee, DD1 4HN, Scotland, UK
[2]School of Life Sciences, University of Dundee, Nethergate, Dundee, DD1 4HN, Scotland, UK
[3]Leibniz Institute of Photonic Technology, Albert-Einstein-Straße 9, 07745 Jena, Germany
[4]School of Physics & Astronomy, Glasgow University, Glasgow, G12 8QQ, Scotland, UK
[5]School of Physics and Medical Imaging, University of Exeter, Stocker Road, Exeter, EX4 4QL, UK
[6]Institute of Scientific Instruments of CAS, Královopolská 147, 612 64, Brno, Czech Republic
[*]Tomas.Cizmar@Leibniz-IPHT.de

Abstract: Digital micro-mirror devices (DMDs) have recently emerged as practical spatial light modulators (SLMs) for applications in photonics, primarily due to their modulation rates, which exceed by several orders of magnitude those of the already well-established nematic liquid crystal (LC)-based SLMs. This, however, comes at the expense of limited modulation depth and diffraction efficiency. Here we compare the beam-shaping fidelity of both technologies when applied to light control in complex environments, including an aberrated optical system, a highly scattering layer and a multimode optical fibre. We show that, despite their binary amplitude-only modulation, DMDs are capable of higher beam-shaping fidelity compared to LC-SLMs in all considered regimes.

OCIS codes: (070.6120) Spatial light modulators; (230.3720) Liquid-crystal devices; (230.4685) Optical microelectromechanical devices; (110.1080) Active or adaptive optics; (060.2350) Fiber optics imaging.

References and links

1. M. J. Booth, M. A. A. Neil, R. Juskaitis, and T. Wilson, "Adaptive aberration correction in a confocal microscope," Proc. Natl. Acad. Sci. U. S. A. **99**(9), 5788–5792 (2002).
2. A. Jesacher, A. Schwaighofer, S. Fürhapter, C. Maurer, S. Bernet, and M. Ritsch-Marte, "Wavefront correction of spatial light modulators using an optical vortex image," Opt. Express **15**(9), 5801–5808 (2007).
3. I. M. Vellekoop and A. P. Mosk, "Phase control algorithms for focusing light through turbid media," Opt. Commun. **281**(11), 3071–3080 (2008).
4. S. M. Popoff, G. Lerosey, R. Carminati, M. Fink, A. C. Boccara, and S. Gigan, "Measuring the transmission matrix in optics: An approach to the study and control of light propagation in disordered media," Phys. Rev. Lett. **104**(10), 100601 (2010).
5. T. Čižmár, M. Mazilu, and K. Dholakia, "In situ wavefront correction and its application to micromanipulation," Nat. Photonics **4**, 388–394 (2010).
6. A. P. Mosk, A. Lagendijk, G. Lerosey, and M. Fink, "Controlling waves in space and time for imaging and focusing in complex media," Nat. Photonics **6**, 283–292 (2012).
7. R. Di Leonardo and S. Bianchi, "Hologram transmission through multi-mode optical fibers," Opt. Express **19**(1), 247–254 (2011).
8. T. Čižmár and K. Dholakia, "Exploiting multimode waveguides for pure fibre-based imaging," Nat. Commun. **3**, 1027 (2012).
9. B. Judkewitz, Y. M. Wang, R. Horstmeyer, A. Mathy, and C. Yang, "Speckle-scale focusing in the diffusive regime with time-reversal of variance-encoded light (TROVE)," Nat. Photonics **7**, 300–305 (2013).
10. E. Papagiakoumou, "Optical developments for optogenetics," Biol. Cell **105**(10), 442–464 (2013).
11. O. Katz, E. Small, Y. Guan, and Y. Silberberg, "Noninvasive nonlinear focusing and imaging through strongly scattering turbid layers," Optica **1**(3), 170–174 (2014).
12. I. M. Vellekoop and A. P. Mosk, "Focusing coherent light through opaque strongly scattering media," Opt. Lett. **32**(16), 2309–2311 (2007).
13. E. G. Van Putten, D. Akbulut, J. Bertolotti, W. L. Vos, A. Lagendijk, and A. P. Mosk, "Scattering lens resolves sub-100 nm structures with visible light," Phys. Rev. Lett. **106**(19), 193905 (2011).

#307073 https://doi.org/10.1364/OE.25.029874
Journal © 2017 Received 14 Sep 2017; revised 2 Nov 2017; accepted 2 Nov 2017; published 15 Nov 2017

Optics EXPRESS

14. D. B. Conkey, A. N. Brown, A. M. Caravaca-Aguirre, and R. Piestun, "Genetic algorithm optimization for focusing through turbid media in noisy environments," Opt. Express **20**(5), 4840–4849 (2012).
15. M. Cui and C. Yang, "Implementation of a digital optical phase conjugation system and its application to study the robustness of turbidity suppression by phase conjugation," Opt. Express **18**(4), 3444–3455 (2010).
16. I. N. Papadopoulos, S. Farahi, C. Moser, and D. Psaltis, "Focusing and scanning light through a multimode optical fiber using digital phase conjugation," Opt. Express **20**(10), 10583–10590 (2012).
17. A. Drémeau, A. Liutkus, D. Martina, O. Katz, C. Schülke, F. Krzakala, S. Gigan, and L. Daudet, "Reference-less measurement of the transmission matrix of a highly scattering material using a DMD and phase retrieval techniques," Opt. Express **23**(9), 11898–11911 (2015).
18. S. Popoff, G. Lerosey, M. Fink, A. C. Boccara, and S. Gigan, "Image transmission through an opaque material," Nat. Commun. **1**, 81 (2009).
19. I. M. Vellekoop, A. Lagendijk, and A. P. Mosk, "Exploiting disorder for perfect focusing," Nat. Photonics **4**, 320–322 (2010).
20. T. Čižmár and K. Dholakia, "Shaping the light transmission through a multimode optical fibre: complex transformation analysis and applications in biophotonics," Opt. Express **19**(20), 18871–18884 (2011).
21. S. Bianchi and R. Di Leonardo, "A multi-mode fiber probe for holographic micromanipulation and microscopy," Lab Chip **12**(3), 635–639 (2012).
22. I. N. Papadopoulos, S. Farahi, C. Moser, and D. Psaltis, "High-resolution, lensless endoscope based on digital scanning through a multimode optical fiber," Biomed. Opt. Express **4**(2), 260–270 (2013).
23. B. R. Brown and A. W. Lohmann, "Complex spatial filtering with binary masks," Appl. Opt. **5**(6), 967–969 (1966).
24. S. N. Chandrasekaran, H. Ligtenberg, W. Steenbergen, and I. M. Vellekoop, "Using digital micromirror devices for focusing light through turbid media," Proc. SPIE **8979**, 897905 (2014).
25. D. B. Conkey, A. M. Caravaca-Aguirre, and R. Piestun, "High-speed scattering medium characterization with application to focusing light through turbid media," Opt. Express **20**(2), 1733–1740 (2012).
26. S. A. Goorden, J. Bertolotti, and A. P. Mosk, "Superpixel-based spatial amplitude and phase modulation using a digital micromirror device," Opt. Express **22**(15), 17999–18009 (2014).
27. D. Akbulut, T. J. Huisman, E. G. V. Putten, and W. L. Vos, "Focusing light through random photonic media by binary amplitude modulation," Opt. Express **19**(5), 4017–4029 (2011).
28. Y. Choi, C. Yoon, M. Kim, T. D. Yang, C. Fang-Yen, R. R. Dasari, K. J. Lee, and W. Choi, "Scanner-free and wide-field endoscopic imaging by using a single multimode optical fiber," Phys. Rev. Lett. **109**(20), 203901 (2012).
29. A. M. Caravaca-Aguirre, E. Niv, D. B. Conkey, and R. Piestun, "Real-time resilient focusing through a bending multimode fiber," Opt. Express **21**(10), 12881–12887 (2013).
30. W. Lee, "Binary computer-generated holograms," Appl. Opt. **18**(21), 3661–3669 (1979).
31. M. Plöschner, T. Tyc, and T. Čižmár, "Seeing through chaos in multimode fibres," Nat. Photonics **9**, 529–535 (2015).
32. J. García-Márquez, V. López, A. González-Vega, and E. Noé, "Flicker minimization in an LCoS spatial light modulator," Opt. Express **20**(8), 8431–8441 (2012).
33. K. J. Mitchell, S. Turtaev, M. J. Padgett, T. Čižmár, and D. B. Phillips, "High-speed spatial control of the intensity, phase and polarisation of vector beams using a digital micro-mirror device," Opt. Express **24**(25), 29269–29282 (2016).
34. M. Persson, D. Engeström, and M. Goksör, "Reducing the effect of pixel crosstalk in phase only spatial light modulators," Opt. Express **20**(20), 22334–22343 (2012).

1. Introduction

Spatial light modulators (SLMs), allowing for precise and dynamic shaping of light beams via computer interface, have opened up numerous new possibilities for photonics in complex environments [1–11]. Amongst other important directions, intense research efforts worldwide exploit SLM-based beam-shaping technologies for improving methods of optical imaging deep inside living tissues. These techniques rely on beam shaping to counteract the effects of natural inhomogeneities which deteriorate light signals propagating through biological samples. Although such signals undergo complex and a priori unpredictable scattering events, their propagation remains deterministic, which in turn enables focusing and imaging through highly complex scattering environments [12, 13].

A range of different wavefront shaping approaches have been developed, including iterative algorithms [12, 14] and time-reversal or phase conjugation [15–17]. These advances have been further complemented by the introduction of the concept of the transmission matrix (TM) [4, 18]. The TM, which can be empirically measured for a given medium, provides complete information about the associated light transport process as a linear relation between a set of input and output spatial light modes, the basis representation of which can be conveniently chosen to suit a

Optics EXPRESS

particular application.

SLMs offer a finite number of spatial degrees of freedom (equal to the number of independently controllable pixels), which dictates the extent to which the complexity of a given medium can be handled, and how efficiently the power of a propagating signal can be utilised. In the so-called ballistic regime, light signals do not deviate significantly from free-space propagation, with changes to propagating wavefronts being commonly described as single-plane phase aberrations. Such light transport can be described by very few propagating modes which can be fully controlled by SLM technology [5] and, in principle, all available optical power can be utilised. In contrast, highly-scattering (e.g. diffusive) media feature a much larger number of allowed spatial modes than the number it is possible to control with SLMs. In this case, only a small fraction of the propagating optical power can be controlled to generate diffraction-limited foci or other optical fields of interest [19]. Finally, there are compelling boundary cases between these extremes, where the number of allowed propagating modes in the system is of the same order as the number of degrees of freedom controllable by SLMs. An example of such an intermediate case is that of light transmission through a multimode optical fibre (MMF). Controlling light transmission through MMFs by digital holography came to the fore only recently [7,8,20–22], opening new perspectives for highly specialised forms of endoscopy, particularly due to a dramatic minimisation of the instrument's footprint and the possibility of diffraction-limited spatial resolution.

Alongside the number of controllable spatial modes (i.e. pixels), there are several other factors determining the achievable performance of digital light shaping technology in various applications. When considering imaging applications, and particularly those relying on the raster scanning of a laser focus inside or behind a complex medium [8, 21, 22], the SLM refresh-rate becomes a vitally important attribute. LC-SLMs have been employed in numerous pioneering experiments involving these forms of imaging but, with refresh rates at 10 - 200 Hz, acquisition of a single frame containing a few kilopixels of data typically takes several minutes [21]. This low frame rate represents a severe obstacle for the majority of possible practical applications. The combination of LC-SLMs with a faster beam-steering technology has been demonstrated to accelerate acquisition rates by over two orders of magnitude, however, this solution significantly compromises the maximum achievable pixel-resolution [8]. Digital micro-mirror devices (DMDs), which are based on micro electro-mechanical systems (MEMS) technology, have therefore emerged as a powerful solution to this problem. Unlike LC-SLMs, which typically modulate the phase of the reflected wavefront with a depth of 8-12 bits, DMDs operate as purely binary amplitude modulators, posing a limit to the precision and efficiency with which each degree of freedom can be controlled [23, 24]. Nevertheless, it has been already shown that using a DMD in the off-axis regime [25, 26] it is possible to measure the TM and to perform beam shaping through both diffusive media [27] and MMFs [28, 29] at very high speeds.

Our study presents a parametric assessment of the performance of LC-SLMs and DMDs as diffractive elements when employed in the ballistic, highly scattering and intermediate regimes. In each case, we quantitatively assess the quality of the generated foci and compare the results side by side. Our results show that surprisingly, in spite of their limited binary amplitude modulation regime, MEMS-based devices outperform the LC analogues not only in speed but also in the fidelity of obtained foci.

2. Methods

To test the performance of LC-based SLMs and DMDs in the ballistic, highly scattering and intermediate regimes, we designed a modular experiment, as shown in Fig. 1. The SLM (DMD/LC-SLM) is illuminated with a highly coherent linearly polarised laser beam at a wavelength of 532 nm, and operates in the off-axis regime so that modulated light is transmitted into the first order of the resulting diffraction pattern. In all presented experiments, for both the LC-SLM and the DMD, an active region was limited to 512×512 pixels. A lens F1a/F1b together with

Optics EXPRESS

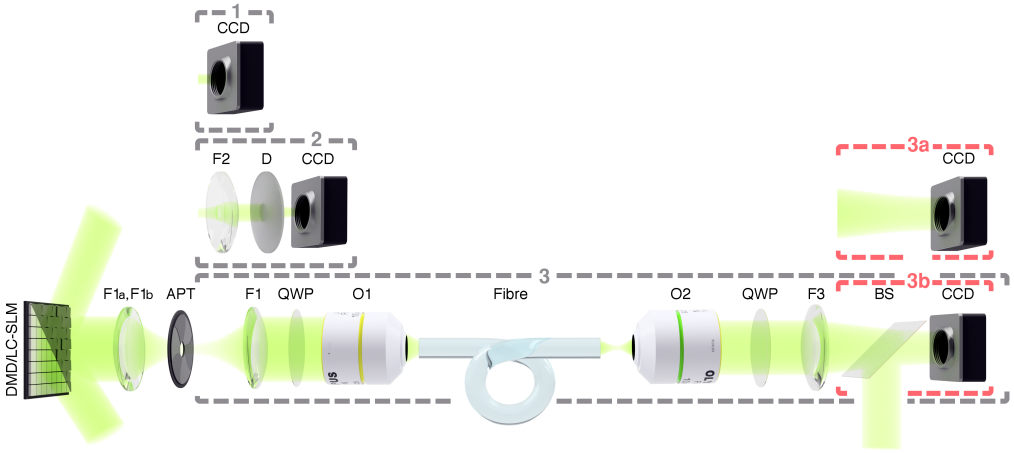

Fig. 1. Modular experimental setup. 1. Ballistic regime. 2. Diffusive regime. 3. MMF with internal(a) or external(b) phase reference. Laser: single-frequency DPSS laser at 532nm (CrystaLaser CL532-075-S); LC-SLM (Meadowlark HSPDM512); DMD (VIALUX V-7001); CCD (Basler pia640-210gm); lenses: F1a (Thorlabs AC254-500-A-ML), F1b (Thorlabs AC254-200-A-ML), F2 (Thorlabs AC254-25-A-ML), F3 (Thorlabs AC254-200-A-ML); APT: iris diaphragm (Thorlabs SM1D12D); QWP: quarter-wave plate (Thorlabs WPQ05M-532); D: ground glass diffuser (Thorlabs DG10-1500-MD); Fibre: 30 cm long 0.22 NA multimode fibre (Thorlabs FG050UGA); O1, O2: microscope objectives (Olympus RMS10X, RMS20X); BS: 50:50 non-polarising beamsplitter (Thorlabs BS004).

an aperture (APT) isolates the first diffraction order, which is aligned with the subsequent optical components. In module 1, the CCD camera placed at the focal plane of the lens (F1a) is employed for the aberration correction experiment in the ballistic regime. Module 2 is used to study the focusing performance in the highly scattering regime. Collimating lens F2, as part of the demagnifying telescope F1a-F2, decreases the beam diameter on the surface of the ground glass diffuser (D) in order to increase the amount of power reaching the camera (CCD). In module 3, the SLM face is reimaged (using F1b and F2 telescope) to the back aperture of the microscope objective O1. The MMF facet is at the focal plane of O1. The microscope objective O2 together with the tube lens F3 project the desired focal plane of the fibre onto the CCD camera. Two quarter-wave plates (QWP) enable the coupling of circularly polarised light into and out of the MMF which has been shown to be better conserved throughout propagation owing to the cylindrical symmetry of the waveguide [31]. Modalities 3a and 3b allow the MMF transmission matrix to be characterised either with an internal phase reference (3a) that has itself been transmitted through the MMF, or with an external reference (3b) provided directly from the laser source via a beam splitter (BS).

As explained elsewhere [5], the wavefront correction technique used here is based on a decomposition of the initial laser field at the SLM plane into a series of orthogonal modes each corresponding to a different square region (subdomain) of the SLM. In our experiments the size of the subdomains was varied from 32×32 down to 4×4 pixels, yielding the number of input modes in the system ranging from 256 to 16386. By modulating a particular subdomain with a grating, one can transfer a part of the reflected optical power from the zeroth diffraction order into the first diffraction order at the Fourier plane. In the case of the LC-SLM, this is achieved using a diagonal blazed phase grating, which for the chosen periodicity of 4 pixels per period (both horizontally and vertically) allowed 42% of the whole optical power to be redirected to the first order. The periodicity of the grating has been chosen in order to avoid overlap of

Optics EXPRESS

different diffraction orders even for the minimum subdomain size used in the experiments. The separation between the neighbouring orders in the Fourier plane has been 4.4 mm and 4.8 mm in the respective cases of LC-SLM and DMD modulators. A binary amplitude grating [30] of the same periodicity of 4 pixels applied in the case of DMD resulted in the efficiency of only 8% under the same conditions. In both cases, applying the grating over a subdomain is equivalent to turning the associated mode 'on' or 'off' as only light directed into the first order is allowed to propagate through the aperture (APT in Fig. 1) into the destination plane. If an internal reference is used, one such mode is selected as the reference and all the remaining modes are examined one by one as follows: A mode under 'test', together with the reference mode, propagates through the optical system and interferes in the destination plane, giving an intensity signal that is monitored by a single CCD pixel. Altering the phase of the tested mode is achieved by laterally translating the grating applied to the corresponding SLM subdomain. Sweeping the phase of the tested mode at a uniform rate results in a sinusoidal time-dependence of the recorded intensity. The phase of this sinusoid reveals the optimal phase at which the tested mode interferes constructively with the reference. Repeating this procedure for all the input modes and then turning all of them 'on' simultaneously with the optimal phase applied, results in optimum focusing as all modes interfere constructively at the same time.

The interferometric measurements of each subdomain were performed with phase-steps of $\pi/2$, and we separately studied the results obtained for a phase sweep of one and two full cycles (i.e. 2π or 4π). Changing the number of cycles in this way allowed us to assess the influence of temporal fluctuations in the efficiency of the modulator during the optimisation procedure. Known sources of temporal fluctuations in LC-SLMs include transfer delay, response time, and flicker [32]. Such fluctuations can affect the accuracy of the interferometric measurements and, in consequence, the quality of the resulting wavefront correction. In our experiments, the issues with transfer delay and response time were mitigated by implementing a waiting time of 50 ms, between uploading the phase hologram and triggering the camera. Additionally, we use a model which is well known to exhibit low, although still apparent, phase flicker. Extending the measurements from one to two periods can improve the accuracy by averaging out these influences, but consequently also doubles the optimisation time.

In the case of the LC-SLM, the bottleneck limiting the time taken to sequentially optimise the phase of all subdomains is the modulator's refresh-rate of 40 Hz. Employing the DMD in place of the LC-SLM reduces the calibration time $\approx 10\times$. In our experiment, the bottle neck is now no longer the modulator itself (as the DMD can operate at up to 22 kHz), but is instead the camera, which can only operate at up to 400 Hz.

The algorithm was implemented on both devices for all three aforementioned regimes of media complexity, the results of which are detailed in the following sections 3-5.

3. Ballistic regime: aberration correction in optical system

Aberrations in optical systems corrupt a propagating wavefront and, in the focal plane, smear out the focus, decreasing its peak intensity. To assess the performance of wavefront correction implemented with the use of both modulator types, we choose the improvement in peak intensity (ratio of peak intensities in the case of corrected and uncorrected wavefronts) as the relative figure of merit to indicate the quality of the focal spot. Figure 2 shows that increasing the number of modes in the wavefront correction algorithm results in enhancement of the peak intensity after the wavefront correction has been applied. The peak intensity is measured at the particular CCD pixel for which the correction has been obtained.

For both modulators, the main cause of the measured aberrations is the curvature of the modulators surfaces. The insets of Fig. 2a and 2b show that the surface of the DMD chip is significantly more curved than that of the LC-SLM. Nonetheless, the wavefront correction technique measures and corrects for these and any other aberrations present in the optical system.

Optics EXPRESS

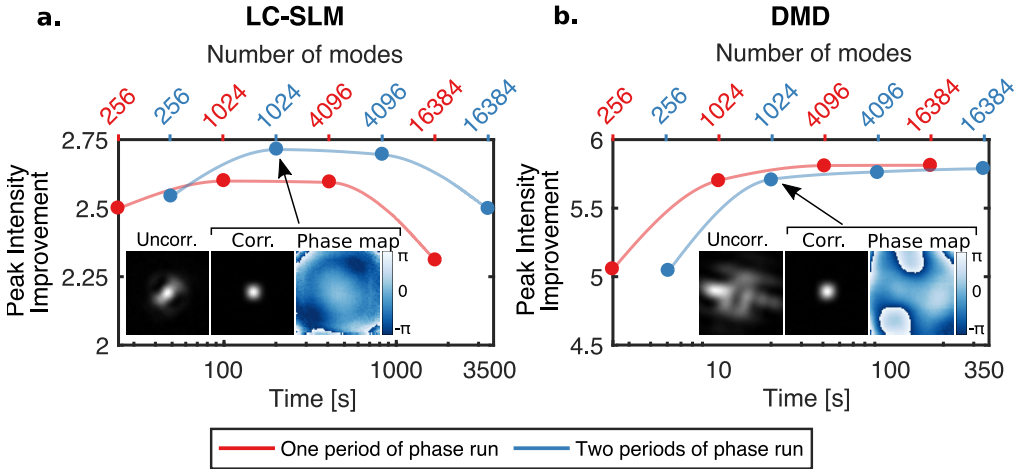

Fig. 2. Ballistic regime. Peak intensity improvement (the ratio of focal point intensity with and without applying the wavefront correction) as a function of optimisation time and number of spatial modes (subdomains) tested, using either an LC-SLM (a) or a DMD (b). The insets show the comparison of uncorrected and corrected focused spots, and the map of the measured phase aberrations in each case. Note that in this specific case the higher values reached using the DMD do not indicate its better performance, rather than much more severe starting conditions – significantly higher curvature of the modulator's surface. The spline interpolations are merely used as the "guide for the eye". The relative standard deviations of the measurements have not exceeded 2%. As they are smaller than the used symbols the error bars are not included in these plots.

Figure 2 shows that when using the LC-SLM, the peak intensity in the focal spot reaches a maximum value when using a correction based upon the measurement 1024 spatial modes (i.e. a 32×32 grid of subdomains). Therefore, in our experiment, this resolution is high enough to accurately capture the majority of the aberrations in the system. However, when the number of spatial modes is increased to 16386 (i.e. a 128×128 grid, with each subdomain consisting of 4×4 LC-SLM pixels), the peak intensity found in the focus begins to fall below the maximum value. This can be understood by considering the scattering in liquid crystals: the portion of light diffracted from such a small subdomain is comparable to the amount of light that is scattered from the rest of the LC-SLM. This relatively strong background signal (with respect to the light reflected of a single subdomain) reduces the accuracy of the measurements. In the most critical case this signal interferes destructively with the reference, which leads to the method's failure in the particular point, thus corrupting the resulting wavefront correction.

In the case of the DMD, the peak intensity found in the focal spot also reaches a maximum after the measurement of 1024 spatial modes, at which point the performance of the system plateaus. As there is less randomly scattered light from the MEMS-based DMD in comparison with the LC-SLM case, further increasing the number of spatial modes does not improve or decrease the performance.

We also tested another aspect of the wavefront correction technique - the effect of increasing the number of phase sweeps from one to two full cycles for each spatial mode under test. In Fig. 2 these measurements are shown in red (one cycle phase sweep) and blue (two cycle phase sweep). In the case of the LC-SLM, increasing the number of phase sweep cycles from one to two leads to an improvement in focal point peak intensity, although of course it also doubles the time taken to perform the measurements. The improvement in peak intensity is more pronounced for larger numbers of spatial modes (i.e. smaller subdomain regions). This behaviour implies that there is a

Optics EXPRESS

random error in the measurements that is more significant for smaller sized subdomain regions and is reduced by averaging over a larger number of measurements. This random error may be due to the 'flicker' associated with LC-SLM operation: LC-SLM devices typically operate by cycling the polarity of the electric field across the liquid crystal layer. Therefore, even when the required pattern is not changed, flicker can occur due to this continuous polarity switching, which periodically alters the phase of each pixel by a small amount. As expected, lack of flicker in the MEMS-based modulator results in no difference in peak intensity for one and two phase sweep cycles.

4. Highly-scattering regime: focusing through a ground glass diffuser

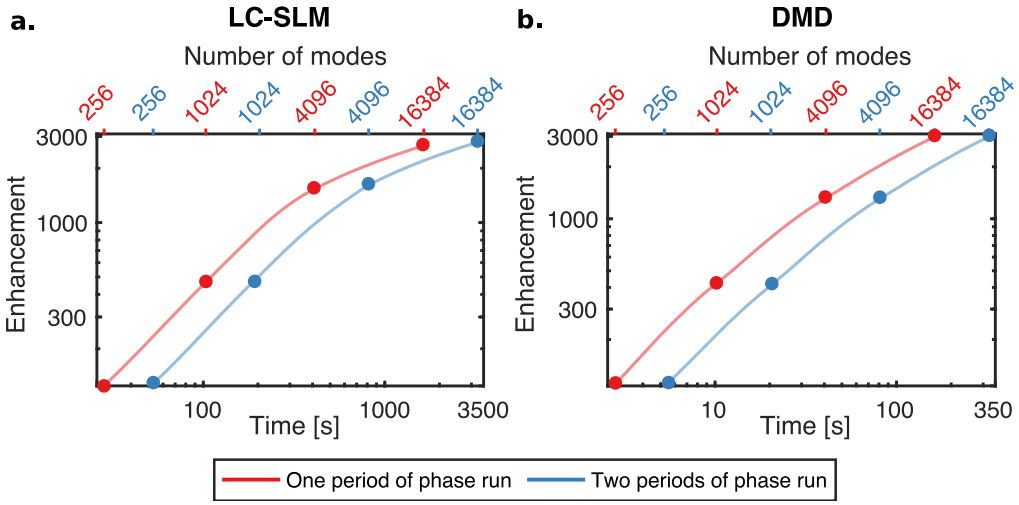

Fig. 3. Highly-scattering regime. Enhancement (the ratio between the optimised peak intensity and the averaged background) as a function of optimisation time and number of spatial modes (subdomains) measured for either an LC-SLM (a) or a DMD (b). The relative standard deviations of the measurements have not exceeded 2%. As they are smaller than the used symbols the error bars are not included in these plots.

For the highly scattering regime, where the medium transforms a coherent beam into a speckle pattern, applying the wavefront correction technique enables redistribution of light towards a chosen target point behind the diffuser. In order to investigate this scenario, the system is set up using module 2 (as shown in Fig. 1) which includes a ground glass diffuser at the Fourier plane of the SLM. In such complex scattering media, the number of channels (i.e. possible separate routes of light propagation) is many times higher than the number of input spatial modes (i.e. subdomains) we can control via an SLM. Therefore, in addition to the chosen target focal spot, this situation also unavoidably leads to the formation of a diffuse background caused by the light we are unable to control. In this case, we use the ratio between the peak intensity at the target point and average background level, referred to here as enhancement, as a comparison metric for this experiment.

Figure 3 shows the enhancement as a function of the number of sampled spatial modes for both the LC-SLM and the DMD modulator. Here the values and trends are similar for both. As in the previous case, measurement using two phase sweep cycles improves the performance for the LC-SLM as it suppresses the adverse effect of phase flicker.

Optics EXPRESS

5. Intermediate regime: focusing through a multimode fibre

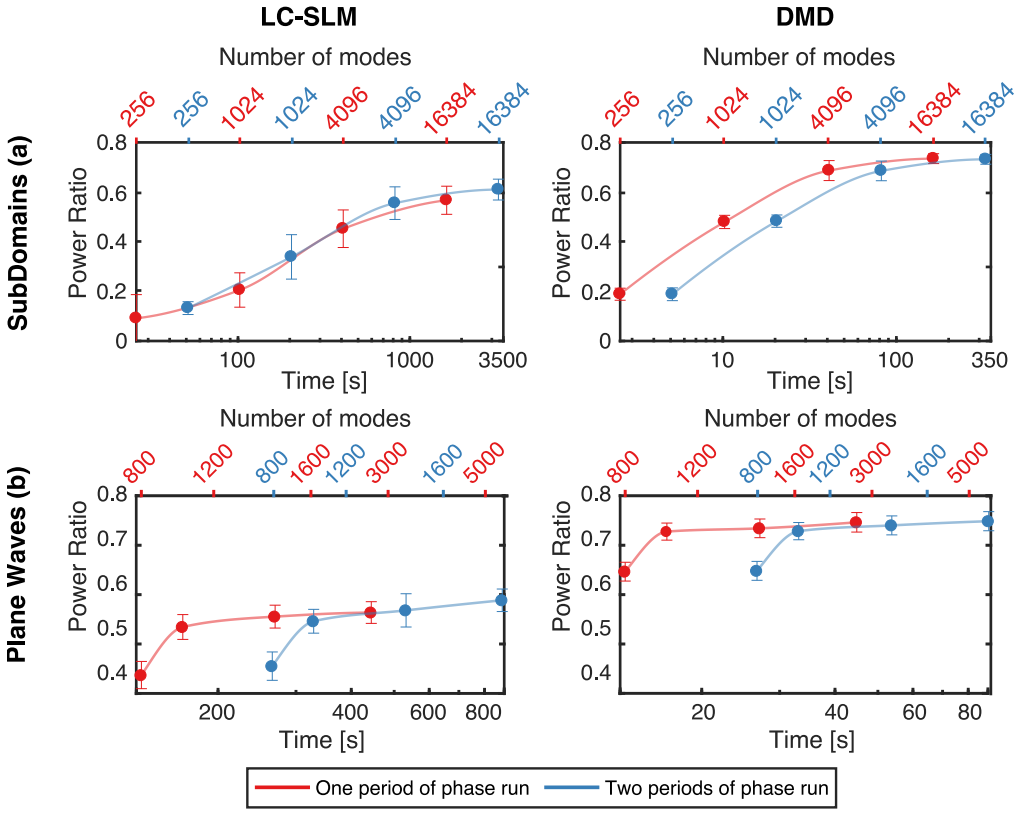

Fig. 4. Intermediate regime: Multimode fibre. Power ratio (the ratio between the power carried by the optimised focus at the distal end of the MMF and the total power leaving the MMF) as a function of optimisation time for both subdomain (a) and Fourier-domain (b) approaches, for either an LC-SLM of a DMD. The error bars have been calculated from three sequential runs of the experimental procedure (measurements of TM) and 7×7 diffraction-limited foci generated across an orthogonal grid at the output facet of the MMF.

5.1. *Subdomain-based optimisation*

The capability of MMFs to deliver almost all of the coupled light to the distal facet renders them a very promising technology for micro-endoscopy, in particular because the same MMF can then collect reflected or fluorescently excited light. In order to compare the performance of the modulators in this case, we use the ratio between the power in the focal spot compared to the full output power emitted from the fibre as a performance metric. Using this power ratio (PR) allows us to roughly estimate the percentage of power contributing to a signal and the one forming the background in the intended application.

The optical setup was as shown in module 3 of Fig. 1 and, in this experiment, we probed the TM in the subdomain basis. Figure 4a shows that in the case of both modulators, the PR starts to reach saturation after measurement of about 4000 spatial modes. However, the PR in the case of the DMD-based system is 10-15% higher for each point on the plot. We believe this is once again due to the detrimental effects of the scattering from liquid crystals in the case of the LC-based modulator, which are not present when using a DMD. During every measurement, and

Optics EXPRESS

when applying a pre-shaped correction wavefront, a portion of this uncontrolled light within the acceptance angle of the fibre propagates towards the distal end and creates an uncontrollable background. We note that it was impossible to directly observe this effect, dealing with normalised values in the first experiment or in the second experiment, where only a small portion of light reflected off the SLM reaches the sensor of the camera.

5.2. Fourier-domain based optimisation

The final experiment was performed exclusively for the case of the MMF, featuring the advantages of the modified fast algorithm presented in [31]. As an alternative to aberration measurement based on the division of the SLM into a grid of subdomains as described in Sec. 2, we investigate the performance of aberration measurement in the Fourier basis. Here, the tested modes are formed by plane waves truncated by the SLM chip, each being transmitted at a different angle corresponding to a specific $\vec{k}$-vector. Each such truncated plane wave forms a focused spot at a different transverse location on the input facet of the MMF. This orthogonal grid of foci forms a new basis of input modes. The distal end of the MMF is imaged on the CCD camera, where the output optical field interferes with an external phase reference. Analogously to the subdomain-based optimisation, for each such input mode, we search for the optimal phase, giving the highest signal at a chosen CCD pixel while interfering with a reference beam. This technique is slightly more demanding in the post-processing stage than the subdomain method, as the reconstruction of the desired wavefront needs to be made in the Fourier domain [31,33]. However, it has the advantage of making a more efficient use of the light transmitted from the SLM during TM measurement: firstly, each measurement involves light reflected from the entire face of the SLM, improving the signal-to-noise ratio of the measurements and, secondly, we only include truncated plane waves which result in focused spots incident within (and therefore coupled into) the fibre core. Ignoring modes that enter the cladding in this way minimises the required number of measurements, therefore significantly decreasing the optimisation time. In order to identify the location of the fibre core, the technique therefore requires a preliminary step: the raster scanning of the fibre facet with focal points, and the measurement of the integrated (total) output power (intensity) at the distal end of the fibre for each input scan position. This enables identification of those spatial modes which can be efficiently coupled through the fibre, defining the size of the basis of input modes for further calibration. Finally, employment of the uniformly distributed external reference signal eliminates the effect of 'blind spots', resulting from the speckled nature of internal references [20]. We implemented this Fourier-based optimisation technique with both modulator types, and now compare their performance in the most relevant scheme for real applications in fibre-based endoscopy.

Figure 4b shows the performance of the Fourier domain-based optimisation for the two modulators. For our fibre, the PR trend plateaus upon the measurement of about 1000 input modes, which coincides with the number of waveguide modes in the fibre per one polarisation state for the given wavelength ($\approx$1000 according to the large V-number approximation). This plateau in PR is reached in approximately one tenth of the time required for the subdomain-based optimisation procedure. Moreover, this improvement in calibration speed does not compromise the performance: maximum PR values are equivalent using either probe basis.

As observed previously in the subdomain-based optimisation, using the Fourier-based optimisation the DMD produces foci at the distal end of the MMF with PR values of up to 15% higher than those generated using an LC-SLM. This is because, despite higher SNR at the measurement stage, the LC-SLM still suffers from a portion of uncontrolled scattered light propagating through the fibre, thus reducing the PR level.

Optics EXPRESS

6. Conclusions

While LC-SLMs have been the standard choice in wavefront-shaping applications for over a decade, and are currently the most frequent choice in complex photonics applications, MEMS-based DMD alternatives have started to gain popularity in the last few years. DMDs are usually chosen because of their faster modulation rates, at the cost of their overall power efficiency.

Our work shows that in the off-axis regime, despite the limited depth of modulation, DMDs may outperform LC-SLMs not only in modulation rate but, importantly, also in beam-shaping fidelity. This opens up the perspective for DMD usage in various applications such as raster-scanning imaging approaches, where the highest possible fidelity is greatly desirable. We have shown that when optimising light transport through complex media, DMD displays have higher beam-shaping fidelity regardless of the complexity of the scattering medium. One reason for this superior fidelity is that DMDs do not suffer from the strong scattering present in LC-SLMs, which corrupts the optimisation procedure and contributes to an uncontrollable background signal. This is especially crucial when focusing light through MMFs, where we have observed that an LC-SLM based system can achieve a power ratio of 60% at the target focal point, while a DMD based system operating in an identical regime reached a power ratio of 75%. In potential applications of this technology to imaging, this translates directly to improvements in image contrast. Another inherent drawback of LC-SLMs is their phase flicker, which decreases the precision of phase measurements during the optimisation procedure. Although this effect can be averaged out by increasing the number of obtained samples for each mode, this results in longer optimisation durations. We note that other possible sources of quality loss, such as cross-talk between pixels, can be expected when using LC-SLMs [34].

In this work, we also demonstrated that when characterising a multimode fibre, using the Fourier-domain based optimisation procedure in place of the subdomain-based approach can decrease the optimisation time by one order of magnitude.

Finally, we emphasise that the diffraction efficiency in the case of the DMD was only 8%, in contrast to 42% for the case of LC-SLM. In many applications this can be compensated for by increasing the power of the laser source; there are however cases where the photon budget cannot be compromised, and the advantages of DMDs would not trade-off well.

Our work could not include all possible means of light modulation frequently used in various regimes, where other choices such as deformable mirrors, ferroelectric LC modulators, piston-like MEMS systems, etc., could outperform both nematic LC-SLMs and DMDs. Our study, however, highlights the importance of careful consideration of parameters in order to reach the optimal balance between speed and performance in wavefront shaping experiments, including several less-recognised differences between LC and MEMS based spatial light modulators commonly used in the field of complex photonics.

Funding

EU FP7 Programme (FP7/2007-2013) REA grant agreement (608133); European Regional Development Fund (CZ.02.1.01/0.0/0.0/15_003/0000476), SUPA PaLS initiative; Royal Academy of Engineering; EPSRC (QuantIC, Grant no. EP/M01326X/1); ERC (TWISTS, grant no. 340507); ERC (LIFEGATE, grant no. 724530).

Acknowledgments

ST and ITL acknowledge support from the EU FP7 Programme. ST, ITL and TČ also acknowledge the financial support of the EU, the "Thüringer Ministerium für Wirtschaft, Wissenschaft und Digitale Gesellschaft", the "Thüringer Aufbaubank" and the Federal Ministry of Education and Research, Germany (BMBF). MJP thanks the Royal Society and the Wolfson Foundation. DBP thanks the Royal Academy of Engineering for support. TČ acknowledges support from the

Optics EXPRESS

European Regional Development Fund-Project "Holographic endoscopy for in vivo applications" (No. CZ.02.1.01/0.0/0.0/15_003/0000476), the SUPA PaLS initiative. This research was also supported by U.K. EPSRC and the ERC.